

# **Effect of Fiber Orientation and Ply Mix on FRP-confined Concrete**

*Principal Investigator: Professor Oral Buyukozturk*

*Graduate Student: Ching Au*

Department of Civil and Environmental Engineering  
Massachusetts Institute of Technology  
Cambridge, MA

*NOTE: For information only.  
Complete research methodology and results  
will appear as journal publication.*

## **Summary**

This work investigates the effects of different fiber orientation and mix of ply configurations on load-deformation behavior and failure modes of FRP confined concrete, with particular emphasis on the kinking phenomenon, which is believed to be a critical physical state from a design standpoint. Within the limitation of the experimental program, the following tentative conclusions have been drawn.

From experimentation, two types of load-deformation behavior were seen on FRP-confined concrete. Type 1, which most often associates with high confinement stiffness and strength, exhibits a system level strain hardening behavior while Type 2, which associates with relatively low confinement properties, shows a system level strain softening behavior. Kinking, which is defined as the point where there is a substantial reduction in axial structural stiffness, signifies structural failure of the concrete core. The kinking point has, in general, a definable graphical relationship with the critical concrete lateral strain. Kink stress appears to shift upward with jacket stiffness and/or thickness. Hoop fibers are efficient in providing confinement, leading to higher kink stress, stiffer post-kinking behavior, and higher ultimate failure stress. However, it also yields brittle failure modes with the release of stored strain energy. Angular fiber jackets tend to yield ductile failure modes with its distinct fiber reorientation mechanism to dissipate energy, although they are not mechanically as efficient in strength enhancement. Ply mix tends to give rise to mixed failure mode and load-deformation behavior. Stack sequence also plays an important role in failure behavior. Further studies in stack sequence in terms of fiber orientation and ply stiffness should be made for a better understanding of the energy dissipation mechanisms during failure.

Comparison of experimental results with several representative confinement models has shown that the existing models are generally capable of describing the overall load-deformation of Type 1 behavior, although a bilinear increase assumption would fail to describe the Type 2 behavior. It is also found that the application of these models to quantify angular fiber wrapped systems is generally sufficient when the equivalent FRP properties in the hoop direction are used.

## 1. Introduction

Column retrofit using fiber-reinforced polymer (FRP) jacketing has been extensively studied in the past decade to explore the effectiveness of this method in strength and ductility enhancement [Saadatmanesh et al 1994, Nanni and Bradford 1995, Mirmiran et al 1996-1998, Watanabe et al 1997, Miyauchi et al 1999, Lam et al 2002] while a large number of projects, both public and private, have made use of such technology, especially in seismically active regions. Yet, most of these studies and applications have focused on the use of fibers only in the hoop direction due to the anticipated strength increase and ease of application. Although some studies have been conducted on the use of angular fibers [Karbhari et al 1993, Howie et al 1995, Picher et al 1996, Mirmiran et al 1996, Hoppel et al 1997], and it has been pointed out that the use of angular fibers could possibly improve failure mode [Howie et al 1995], the effects of fiber orientation and stack sequence are generally not well understood. Also, extensive efforts have been made to develop ultimate strength models for FRP wrapped columns [Lam et al 2002], but the structural significance of the ultimate state in terms of design and safety might not be as critical as that of the kinking point where there is a sharp reduction in slope in the load-deformation curve at about where the unconfined concrete exhibits failure [Howie et al 1995].

The objective of this study is to explore the use of different fiber orientation and mix of ply configurations in attaining a range of load-deformation behavior and failure modes, from which improved physical insights into kinking phenomenon, fiber response, and ply interactions can be gained as a basis for behavioral enhancement for strength as well as ductility at failure of these systems. Experimental results are compared to existing stress-strain models for assessing their performance in quantifying the load-deformation behavior of cylindrical concrete passively confined by various angular fiber wrap configurations.

## 2. Experimental Work

### 2.1 Specimens

A total of twenty-four 150 mm x 375 mm concrete cylindrical specimens were tested, of which eighteen were FRP-wrapped while six were unwrapped control specimens. The 375 mm cylinder height was chosen based on the reported phenomenon that three-dimensional stress states would extend from the end surface to a distance of about 0.86 times the diameter of the cylinder [van Mier 1984] resulting from the elastic mismatch between the steel loading platens and the concrete cylinder. Thus for this research, cylindrical specimens with an aspect ratio of 2.5 was chosen so that an approximately 120 mm zone of the specimens at mid-height would be under uniaxial compression and free from 3-dimensional stress effects from the ends. Concrete cylinders were vertically cast and had an average 28-day characteristic compressive strength of 24.2 MPa with a standard deviation of 2.2 MPa (from 150 mm x 375 mm cylinders).

FRP fabrics made of E-glass fibers, impregnated in an ambient-cured 2-part epoxy matrix, that were obtained from a U.S. manufacturer as commercially available systems, were used throughout this study. Three types of fabrics were employed to produce six wrap configurations. Designations for  $0^\circ$  hoop,  $0^\circ/90^\circ$  hoop/vertical, and  $\pm 45^\circ$  bi-angular fabrics were respectively UC, W, and WA, as illustrated in Figure 1. UC fabric consisted of unidirectional fiber roving densely placed in the  $0^\circ$  direction with additional sparsely spaced glass fibers in the  $90^\circ$  direction for linking purposes. W fabrics consisted of  $0^\circ/90^\circ$  bi-directional weaved fibers with equal fiber content running in both directions. WA fabrics also consisted of bi-directional weaved fibers

with equal fiber content in both directions but they were oriented in  $\pm 45^\circ$ . Respective tensile properties and laminate thickness are summarized in Table 1.

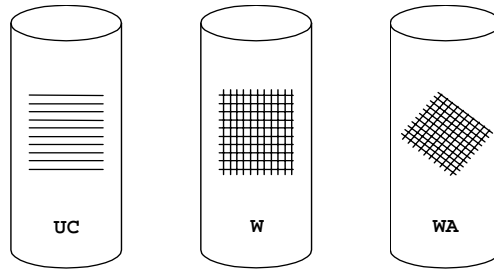


**Figure 1. Basic Fabric Designation**

	UC	W	WA
0° (Hoop) Tensile Strength, MPa	575.0	309.0	279.0
0° (Hoop) Tensile Modulus, GPa	26.1	19.3	18.6
Elongation at break, %	2.2	1.6	1.5
90° (Vertical) Tensile Strength, MPa	21.0	309.0	279.0
Laminate thickness, mm	1.3	0.3	0.9

**Table 1. FRP Fabric Properties**

The ambient-cured 2-part epoxy had a tensile strength of 72.4 MPa and a tensile modulus of 3.2 GPa. Elongation at break was 5%. Mix ratio (Part A to Part B) was 100 to 34.5 by weight.

Six wrap configurations were designed. Three identical specimens for each configuration were prepared and tested to ensure data consistency. Wrap configurations are summarized in Table 2. Each designation is read from left to right, corresponding to the layers from inside out. The number that immediately follows the letter C, meaning cylindrical specimens, shows the total number of wraps used for the specimen. The number that immediately follows any one of the fabric designations (UC, W, or WA) shows the number of plies of that particular type of fabric.

Configuration	Designation	Description
1	C1-UC1	1 layer of UC fabric
2	C1-W1	1 layer of W fabric
3	C1-WA1	1 layer of WA fabric
4	C2-W1-WA1	1 inner layer of W + 1 outer layer of WA
5	C2-UC1-WA1	1 inner layer of UC + 1 outer layer of WA
6	C2-WA1-UC1	1 inner layer of WA + 1 outer layer of UC

**Table 2. Wrap Configurations**

All confined cylinders were wrapped using the wet lay-up technique after the plain concrete cylinders were primed using thickened epoxy. Proper fabric alignment was visually inspected. A 75 mm lap joint was used and was found to be sufficient from preliminary tests for stress transfer for the given fabric and adhesive systems. A final coat of epoxy was applied to the wrapped specimens for complete saturation. The FRP jackets were then ambient cured for at least 72 hours.

## 2.2 Instrumentation and Loading

All specimens were instrumented with extensometers and linear variable differential transducers (LVDT). Three clip-on extensometers that were mounted 120° apart on the specimens were used to monitor axial strains at mid-height. Two additional vertical LVDT were placed 180° apart close to the cylinders to monitor axial displacements between the loading platens. One of the LVDT was always placed next to the lap joint for referencing. Two specially designed LVDT mounting spring systems were mounted 90° apart within the 120 mm mid-height range to monitor radial strains in the horizontal plane.

## 2.3 Test Results

Load-deformation behaviors, which are captured by both axial shortening and radial dilatation, are shown in Figure 2. For visual clarity, only one set of curves (axial and lateral behavior) that represents a wrap configuration is included in each plot. Each set shown resulted from testing of one specimen. All three tested specimens within each wrap configuration yielded consistent data. Axial strain data used for plotting were obtained from average measurements from the three extensometers for each specimen. Lateral strain data were obtained from average readings for each specimen from the two spring-loaded lateral LVDT devices. Maximum stress and the associated strains for the respective configurations are summarized in Table 3. Strength increase is computed and ranked.

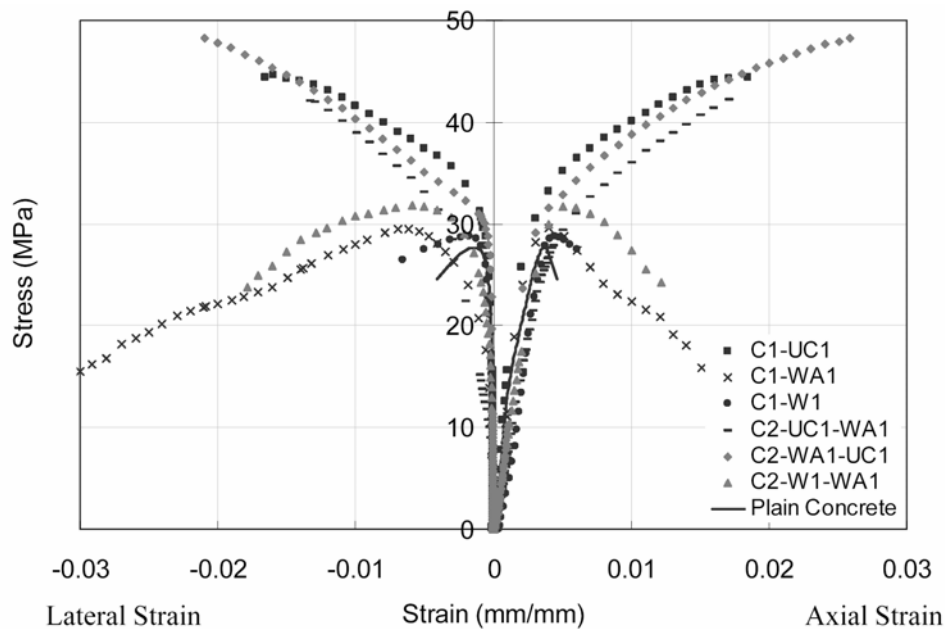


Figure 2. Selected Load-Deformation Plots of Each Configuration

Strength Rank	Designation	Peak Stress Average, MPa	Strain at Peak Stress Average, mm/mm		Ultimate Strength Increase Average, %
			Axial	Lateral	
1	C2 – WA1 – UC1	48.2 (0.55)	0.0260 (0.001021)	0.0221	99
2	C1 – UC1	43.8 (0.90)	0.0163 (0.003028)	0.0148	81
3	C2 – UC1 – WA1	42.6 (3.89)	0.0166 (0.000922)	0.0148	76
4	C2 – W1 – WA1	31.8 (0.73)	0.0055 (0.000680)	0.0056	32
5	C1 – W1	29.8 (1.19)	0.043 (0.001202)	0.0038	23
6	C1 – WA1	27.0 (2.83)	0.0050 (0.000922)	0.0076	12
7	Unconfined	24.2 (2.20)	0.0036 (0.000192)	0.0015	–

*Standard deviations are indicated as values in parentheses.*

**Table 3. Summary of Peak Stress, Peak Strains, and Strength Increase**

### 2.3.1 Observed Load-Deformation Behavior

As observed from Figure 2, the obtained load-deformation responses consist of two main types. Figure 3 shows banded plots in which shaded bands are drawn on top of the stress-strain curves shown in Figure 2 to clearly illustrate the two trends of responses. Note that both single-ply and mixed-ply strengthened specimens could fall within either band.

Type 1 load-deformation demonstrates a system level strain hardening with a distinct bilinear behavior in which a reduction in stiffness is experienced after axial stress has reached a level somewhat higher than the unconfined cylindrical concrete strength. The point at which significant axial stiffness reduction begins is referred to as the kinking point, as termed by Howie et al (1995). Beyond kinking, there is a steady increase in stress until the wrapped concrete system fails entirely. Failure of Type 1 often involves explosive fiber fracture in the jacket accompanied by concrete crushing in the core. Note also that Type 1 behavior always associates with configurations consisting of hoop fibers, which are stiffer and stronger than the other two fiber types used (see Table 1).

Type 2 load-deformation is similar to that of unconfined concrete, except that the peak stress is somewhat higher and that the post-peak straining is much larger as the fractured concrete is contained. A system level strain softening is observed after the peak stress. Note that the peak stress also represents the point at which a change in stiffness occurs, it is termed here the kinking point as well for the purposes of subsequent discussions. Kinking in Type 2 specimens occurs at a somewhat higher level compared to unconfined concrete, but is generally not as high as that in Type 1. Type 2 is seen to associate with bi-directional fibers, which have both lower stiffness and strength than unidirectional fibers in our case. Post-peak straining is particularly pronounced with the use of angular fibers (see Figure 2). This is demonstrated by the much longer descending tails of the stress-strain curves, signifying a steady decrease in strength without fiber rupture in the jacket. The intact jacket resulted in a high level of physical containment after peak stress is reached, at which fiber reorientation and stretching in the WA fabric started to become obvious. Damaged concrete are well confined until the tests were stopped. Large inclined cracks are, however, seen in the core upon examination after tests. The equivalent fabric stiffness, as computed from the rule of mixtures in laminate theory, associated with Type 2 is lower than that

in Type 1, regardless of the number of plies. As such, Type 2 behavior is observed with relatively low confinement stiffness.

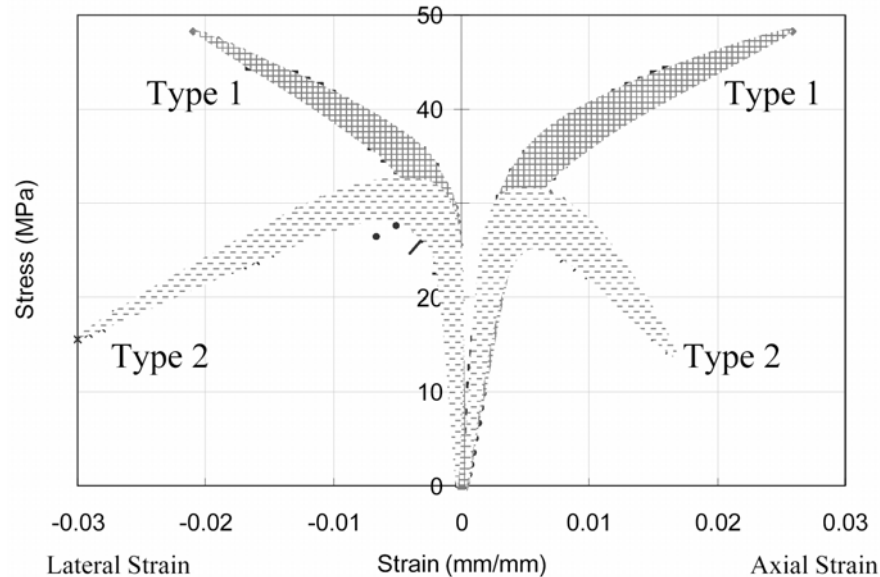


**Figure 3. Banded Plots of Load-Deformation Behavior**

### 2.3.2 Observed Failure Modes

At the failure state where system failure was declared by the sudden reduction in load resistance, both brittle and ductile behaviors were observed from the six configurations, although all six but one showed structural ductility in the form of system-level strain hardening and strain softening before their respective failure points. C1-W1 was the only configuration that did not show ductility during loading and at failure.

Brittle failure state was seen with hoop fiber fracture and hence was associated with all Type 1 load-deformation specimens, namely, C1-UC1, C2-UC1-WA1, and C2-WA1-UC1. In addition, C1-W1 also exhibited brittle failure due in part to hoop fiber rupture, as will be discussed in more detail below, although it showed a Type 2 load-deformation behavior. In this case, the fiber rupture was probably due to low fabric strength, which led to jacket failure before further strength enhancing confinement could be developed.

Angular fiber wrap configurations appear to produce a ductile failure state where fiber reorientation occurred in place of fiber fracture that was seen in the case of Type 1. Post-peak straining was substantial both in the axial and radial directions. Tendency of angular fiber reorientation to align with hoop stress direction was noted. This reorientation allowed a relatively compliant radial dilatation, accommodating slippage between cracked concrete inside the containment jacket without rupturing the fibers. This type of failure mode was seen on C1-WA1 and C2-W1-WA1, which both gave rise to Type 2 load-deformation behavior.

***Brittle Failure State (Figures 4 – 9)***  
***C1-UC1 (1 layer of UC fabric)***



**Figure 4. Failure of C1-UC1**

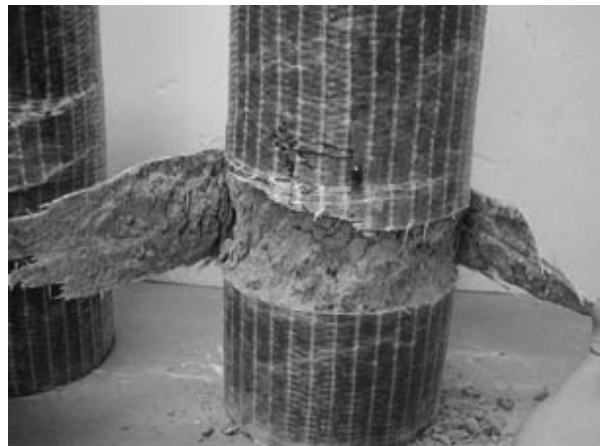


**Figure 5. Localized Damage Zone of C1-UC1**

*C2-UC1-WA1 (1 inner layer of UC + 1 outer layer of WA)*



**Figure 6. Failure of C2-UC1-WA1**

*C2-WA1-UC1 (1 inner layer of WA + 1 outer layer of UC)*



**Figure 7. Failure of C2-WA1-UC1**

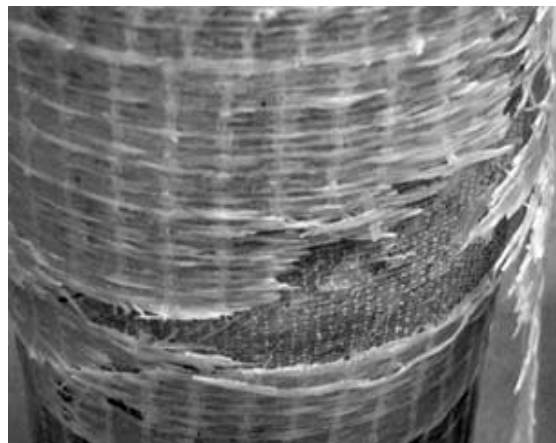


**Figure 8. Delamination Between Inner WA and Outer UC Layer**

*C1-W1 (1 layer of W fabric)*

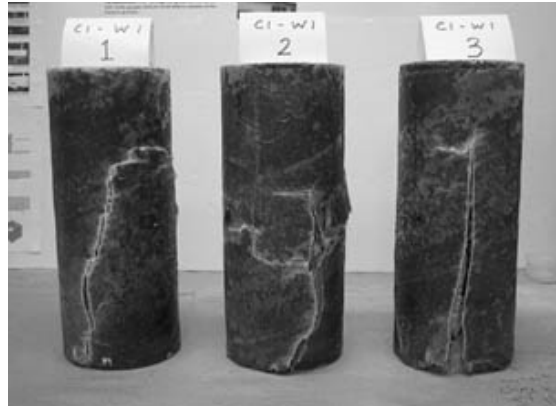


**Figure 9. Failure of C1-W1**

***Ductile Failure State (Figures 10 – 13)***  
*C1-WA1 (1 layer of WA fabric)*



**Figure 10. Failure of C1-WA1**



**Figure 11. Fiber Reorientation**



**Figure 12. Global Concrete Shear Crack**

*C2-W1-WA1 (1 inner layer of W + 1 outer layer of WA)*

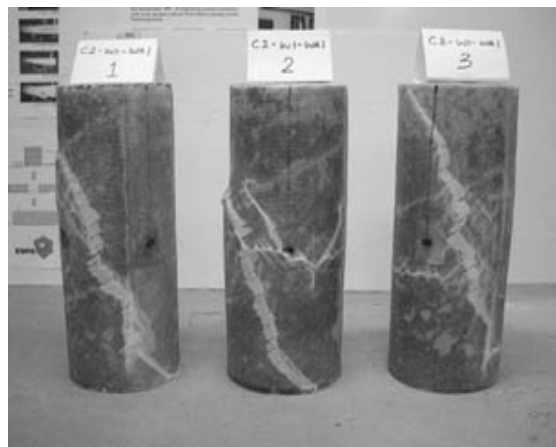


**Figure 13. Failure of C2-W1-WA1**

### **3. Discussion**

#### **3.1 Kinking Phenomenon**

Two types of load-deformation behavior beyond kinking can take place – either strain hardening (Type 1) or strain softening (Type 2). In either case, however, a stiffness reduction is experienced as compared to the pre-kinking stiffness. This significant reduction in axial stiffness must imply the failure of concrete core since FRP jacket still remains intact. Starting from the kink point, further increase in external load results in a more compliant axial behavior. In other words, kinking represents the structural failure of concrete in a cylindrical confined concrete system. In terms of design, the kink stress is of paramount importance. Note that the use of design strength beyond the kink stress for a given jacketed system is yet to be justified, especially for loading cases other than uniaxial compression. As such, there is a need to define

precisely the kinking stress level, especially for those jacketed systems that give rise to a transitive kinking region where a clear kink point cannot be easily identified.

### 3.2 Effect of Fiber Orientation on Kink Stress

Fiber orientation has significant effect on the fabric stiffness in the hoop direction in a FRP jacket. Larger is the fiber-load alignment deviation lower is the equivalent fabric stiffness [Peters 1998]. A higher jacket stiffness in the hoop direction will result in a higher confinement pressure and hence a higher kink stress due to the reasons discussed earlier. Assuming that both concrete and FRP materials behave elastically up to the kink stress and that the bond between the two materials is intact, it can be derived from equilibrium and compatibility that the confinement pressure be related to the axial stress as follows:

$$(1) \sigma_p = \nu_c \frac{E_{FRP}(\theta)t_{FRP}}{E_c R} \sigma_a$$

where  $\sigma_p$  is the confinement pressure,  $\sigma_a$  the external axial stress,  $E_{FRP}(\theta)$  the FRP elastic modulus as a function of  $\theta$ , the fiber-hoop stress alignment deviation,  $t_{FRP}$  the FRP jacket thickness,  $E_c$  the concrete tangent modulus,  $\nu_c$  the concrete Poisson's ratio, and  $R$  the column radius. From the rationale developed before,

$$(2) f_A = f(\sigma_p, f'_{co})$$

where  $f'_{co}$  is the concrete strength. Hence,  $f_A$  is also a function of  $E_{FRP}(\theta)$ , although the precise relation requires further investigation. But it must be true that a stiffer FRP jacket will give rise to a higher kink stress. In other words, the use of hoop fibers is efficient in upshifting the kink stress level.

## 4. Comparison of Results with Existing Confinement Models

While the use of angular fibers and/or mix plies has shown some promise in improving ductility during the post-peak state and at the failure state, proper design of such retrofitted cylindrical concrete structures requires accurate modeling of the load-deformation behavior. In this work, the performance of three representative existing confinement models was therefore evaluated in view of the findings from this investigation. Refer to the studies by Karbhari and Gao (1997), Samaan et al. (1998), and Miyauchi et al. (1999).

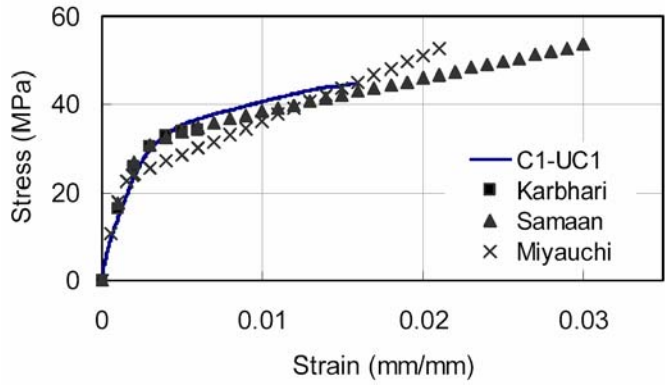


Figure 14. Experimental and Analytical Plots (C1-UC1)

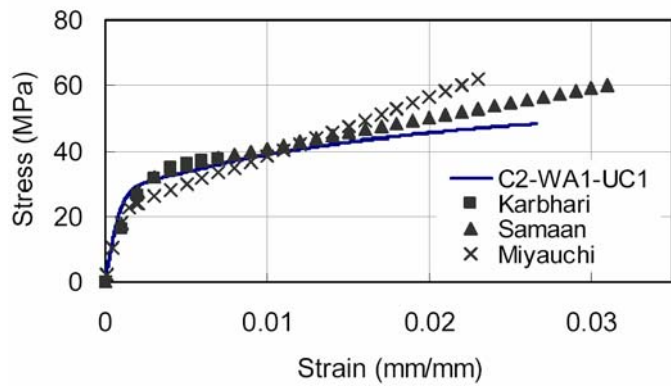


Figure 15. Experimental and Analytical Plots (C2-WA1-UC1)

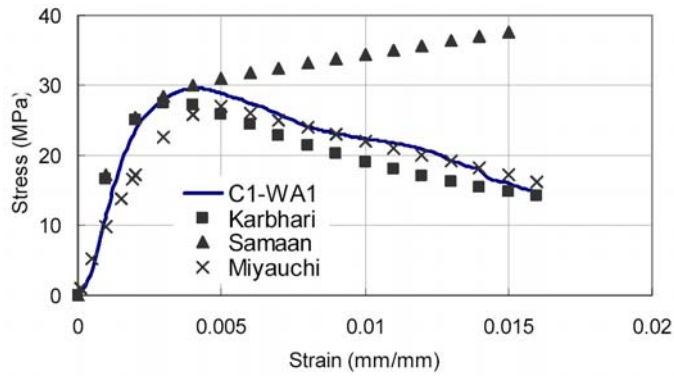


Figure 16. Experimental and Analytical Plots (C1-WA1)

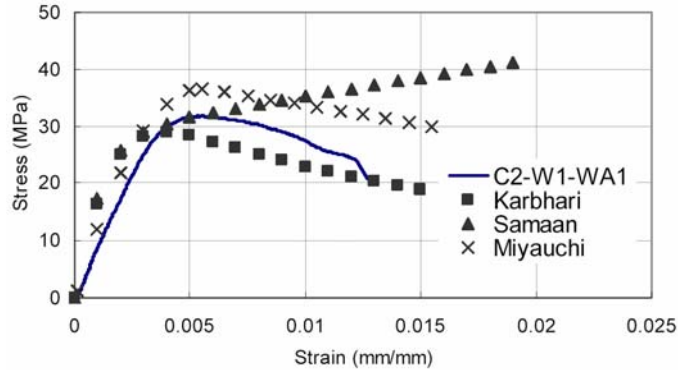


Figure 17. Experimental and Analytical Plots (C2-W1-WA1)

## 5. References

- American Society for Testing and Materials (2003). "Standard Practice for Capping Cylindrical Concrete Specimens - ASTM C617." *ASTM Standards*.
- American Society for Testing and Materials (2003). "Standard Test Method for Compressive Strength of Cylindrical Concrete Specimens - ASTM C39." *ASTM Standards*.
- Hoppel, C. P. R. and Bogetti, T. A. G. (1997). "Design and Analysis of a Composite Wraps for Concrete Columns." *J. Reinforced Plastics and Composites*, Vol.16, No.7, 588-602.
- Howie, I. (1995). *A Study on the Use of Composite Wraps for Rehabilitation of Deteriorated Concrete Columns*, Master Thesis, University of Delaware.
- Howie, I. and Karbhari, V. M. (1995). "Effect of Tow Sheet Composite Wrap Architecture on Strengthening of Concrete Due to Confinement: I – Experimental Studies." *J. Reinforced Plastics and Composites*, V.14, Sept., 1008-1030.
- Karbhari, V. M., Eckel, D. A., and Tunis, G. C. (1993). "Strengthening of Concrete Column Stubs through Resin Infused Composite Wraps." *J. Therm. Comp. Mat.*, V.6, 92-106.
- Karbhari, V.M. and Gao, Y. (1997). "Composite Jacketed Concrete Under Uniaxial Compression – Verification of Simple Design Equations." *J. Mat. In Civil Engng.*, 185-193.
- Lam, L. and Teng, J. G. (2000). "Strength Models for FRP-confined Concrete." *J. Struct. Engg.*, ASCE, Vol.128, No.5, May, 612-623.
- Mirmiran, A., Kargahi, M., Samaan, M., and Shahawy, M. (1996). "Composite FRP-Concrete Column with Bi-directional External Reinforcement." *Fiber Composites in Infrastructure: Proceedings of the First International Conference in Composites in Infrastructure ICCI '96*.
- Mirmiran, A. and Shahawy, M. (1997). "Dilation Characteristics of Confined Concrete." *Mech. Of Cohesive-Frictional Mat.*, V.2, 237-249.
- Mirmiran, A. and Shahawy, M. (1997). "Behavior of Concrete Columns Confined by Fiber Composites." *J. Struct. Engg.*, V.123, No.5, 583-590.
- Mirmiran, A., Shahawy, M., Samaan, M., Echary, H. E., Mastrapa, J. C., and Pico, O. (1998). "Effect of Column Parameters on FRP-Confined Concrete." *J. Comp. for Const.*, V.2, No.4, Nov., 175-185.
- Miyauchi, K., Inoue, S., Kuroda, T., and Kobayashi, A. (1999). "Strengthening Effects of Concrete Column with Carbon Fiber Sheet." *Transactions of the JCI*, V.21, 143-150.
- Nanni, A. and Bradford, N. M. (1995). "FRP Jacketed Concrete Under Uniaxial Compression." *Const. & Building Mat.*, V.9, No.2, 115-124.

- Neville, A. M. (1973). *Properties of Concrete*, John Wiley and Sons.
- Peters, S. T. (editor). (1998). *Handbook of Composites*, 2<sup>nd</sup> Edition, Chapman and Hall.
- Picher, F., Rochette, P., and Labossiere, P. (1996). "Confinement of Concrete Cylinders with CFRP." *Fiber Composites in Infrastructure: Proceedings of the First International Conference on Composites in Infrastructure, Tuscon, Jan.*, 829-841.
- Saadatmanesh, H., Ehsani, M. R., and Li, M. W. (1994). "Strength and Ductility of Concrete Columns Externally Reinforced with Fiber Composite Straps." *ACI Struct. J.*, V.91, No.4, July-August, 434-447.
- Samaan, M., Mirmiran, A., and Shahawy, M. (1998). "Model of Concrete Confined by Fiber Composites." *J. Struct. Engg.*, V.124, No.9, Sept., 1025-1031.
- van Mier, J. G. M. (1984). "Complete Stress-strain Behavior and Damaging Status of Concrete Under Multiaxial Conditions." *RILEM/CEB Symposium on Concrete Under Multiaxial Conditions*, INSA, Toulouse, May, Session 3.
- Watanabe, K., Nakamura, H., Honda, Y., Toyoshima, M., Iso, M., Fujimaki, T., Kaneto, M., Shirai, N. (1997). "Confinement Effect of FRP Sheet on Strength and Ductility of Concrete Cylinders Under Uniaxial Compression", *Proceedings of the Third International Symposium – Non-Metallic (FRP) Reinforcement for Concrete Structures*, V.1, 233-240.

## 6. Nomenclature

$E_c$	concrete tangent modulus
$E_{FRP}$	FRP elastic modulus
$R$	column radius
$f_A$	kink stress
$f_c$	confined concrete axial stress
$f_{FRP}$	tensile strength of FRP
$f_{cc}'$	peak confined concrete strength
$f_{co}'$	concrete compressive strength
$t_{FRP}$	FRP jacket thickness
$\varepsilon_c$	confined concrete axial strain
$\varepsilon_{cc}$	ultimate confined concrete axial strain
$\varepsilon_{co}$	critical axial strain of unconfined concrete
$\varepsilon_{cr}$	critical lateral strain of unconfined concrete
$\theta$	fiber-hoop stress alignment deviation
$\nu_c$	concrete Poisson's ratio
$\sigma_a$	external axial stress
$\sigma_p$	confinement pressure